A crossed molecular beams investigation of the reactions $O(^3P) + C_6H_6$, C_6D_6

Steven J. Sibener,[a] Richard J. Buss, Piergiorgio Casavecchia,[b] Tomohiko Hirooka,[c] and Yuan T. Lee

Materials and Molecular Research Division, Lawrence Berkeley Laboratory, and Department of Chemistry, University of California, Berkeley, California 94720
(Received 29 October 1979; accepted 2 January 1980)

A crossed beams investigation of the reactions of $O(^3P) + C_6H_6$, C_6D_6 has beeen carried out using a seeded, supersonic, atomic oxygen nozzle beam source. Angular and velocity distributions of reaction products have been used to identify the major reaction pathways. The initially formed triplet biradical, C_6H_6O (C_6D_6O), either decays by hydrogen (deuterium) elimination or becomes stabilized, most likely by nonradiative transition to the S_0 manifold of ground state phenol. CO elimination was not found to be a major channel. The branching ratio between H(D) atom elimination and stabilization was found to be sensitive to both collision energy and isotopic substitution.

INTRODUCTION

The reactions of ground state oxygen atoms with both aliphatic and aromatic hydrocarbons are of considerable interest because they are important in combustion processes, atmospheric chemistry, and photochemical air pollution. A relatively large number of kinetic studies have been reported for oxygen atom reactions with alkanes and alkenes in which reaction rate constants have been determined. Gutman and co-workers have recently used crossed molecular beams employing photoionization mass spectrometry to identify the elementary reaction products resulting from oxygen atom reactions with various alkenes and alkynes.[1-3] In contrast to the above, atomic oxygen reactions with aromatic hydrocarbons have not been extensively studied. The simplest reactions of this class [$O(^3P)$ + benzene and toluene] are the only atom–aromatic hydrocarbon reactions that have been studied by a variety of techniques. Relative reaction rates for the $O(^3P)$ + benzene reaction have been determined using static photolysis techniques.[4,5] Absolute reaction rate constants for the $O(^3P)$ + benzene reaction have been determined using pulsed radiolysis,[6] discharge flow,[7-9] modulation-phase shift,[10,11] and flash photolysis–NO_2 chemiluminescence[12] techniques. In spite of these studies, very little information is available on the actual elementary reaction products arising from the bimolecular reaction of atomic oxygen with benzene, and, consequently, the reaction mechanism is poorly understood.

Product identification is severely complicated in the above gas phase studies by the presence of viscous, nonvolatile reaction products which are possibly polymeric in character.[4,8] These nonvolatile products indicate that some of the initial elementary reaction products are highly reactive species which probably undergo rapid secondary reaction. The major volatile reaction product which has been consistently observed is phenol, which accounts for about 10%–15% of the oxygen atom consumption in these studies.[4,8,13,14] Phenol has been shown to account for more than 95% of the volatile products which result when this reaction is studied at atmospheric pressure.[8] Carbon monoxide has also been reported as a reaction product.[4] In an attempt to identify the elementary reaction products Sloane[15] has carried out a simple crossed beam experiment, employing effusive beams and a nonrotatable mass spectrometer, in which phenol production and carbon monoxide elimination, possibly yielding 3-pentene-1-yne, were reported as the two open reactive pathways. It is apparent from the above discussion that there is still considerable uncertainty about the elementary reaction products which arise from the electrophilic attack of oxygen atoms on benzene, which serves as the model system for understanding oxygen atom–aromatic ring reactions.

This paper describes the results from a series of well-defined crossed molecular beam experiments which have been carried out under single collision conditions in our laboratory to elucidate the reaction dynamics and energetics of the $O(^3P)$ + benzene reaction. The reaction has been studied as a function of both collision energy and isotopic substitution in order to clarify the factors which dominate the reaction dynamics. Differential reactive angular distributions accompanied with velocity analysis of the reaction products at several laboratory angles have contributed to our understanding of the elementary reaction pathways which are operative. In particular, these studies make use of a novel and important feature which is inherent in crossed beam experiments employing rotating mass spectrometer detectors: the ability to identify unambiguously the primary polyatomic reaction products resulting from bimolecular reactive collisions by using the dynamic and energetic constraints which are imposed on the reaction products. These experiments are especially well suited for studying reactions involving polyatomic species since parent–daughter ion pairs created in the electron bombardment ionizer of the detector must have identical angular and velocity distributions, while reaction channels involving different dynamics (e.g., substitution versus additional reactions)

[a] Present address: Bell Laboratories, 600 Mountain Avenue, Murray Hill, N. J. 07974.
[b] Permanent address: Dipartimento di Chimica dell' Università, 06100, Perugia, Italy.
[c] Permanent address: Department of Chemistry, Faculty of Science, The University of Tokyo, Hongo, Tokyo 113, Japan.

 0021-9606/80/084341-09$01.00

are clearly distinguishable by their angular and velocity distributions. In contrast to this, traditional gas phase studies which use nonrotatable mass spectrometric particle detection for product identification are frequently complicated by the fragmentation of parent polyatomic species in the electron bombardment ionizers of these systems. This is particularly a problem when high vibrationally excited polyatomic species are ionized by electron bombardment as the parent ion mass peak may be of very low intensity relative to its daughter peaks. For example, the observation of $m/e = 66$ ($C_5H_6^+$) in the $O(^3P)$ + benzene reaction is not in itself sufficient to differentiate between phenol fragmentation during ionization and actual CO elimination. In this study we have made extensive use of product angular distributions to unravel the primary reaction channels of the $O(^3P)$ + benzene reaction.

EXPERIMENTAL

The crossed beam apparatus used in these studies was similar in design to one which has been previously described.[16] Briefly, two beams which are doubly differentially pumped are crossed at 90° in a scattering chamber which has a pressure of $\sim 1\times10^{-7}$ Torr. The main scattering chamber is pumped by a 5300 l/s diffusion pump and by a liquid nitrogen cooled cold shield which is very effective in pumping condensable gases. Particles which are scattered in the plane defined by the two colliding beams are detected by a triply differentially pumped quadrupole mass spectrometer which rotates about the intersection point of the two beams. The incident neutral particles are ionized in the detector by an electron bombardment ionizer which is operated with an electron energy of 200 eV.

The seeded, supersonic atomic oxygen beams used in these studies were generated by a high pressure, radio frequency discharge beam source which has been described in detail elsewhere.[17,18] The high energy atomic oxygen beam was generated by discharging a 10% O_2 in helium gas mixture at 110 Torr total pressure by 130 W of rf power. The resulting fast atomic oxygen beam had a measured peak velocity of 1.95×10^5 cm/s and a Mach number of 5.8, which corresponds to a FWHM velocity spread of 29%. The beam of oxygen seeded in helium is known to contain a small amount of $O(^1D)$[18] but the reaction $O(^1D) + C_6H_6$ is not expected to alter the main features of $O(^3P) + C_6H_6$ because the large cross section ~ 7 Å^2,[5] and much greater $O(^3P)$ concentration will make the latter reaction dominate. Molecular dissociation was about 55% under these operating conditions. The low energy atomic oxygen beam was generated by discharging a 10% O_2 in argon gas mixture at 250 Torr total pressure by 195 W of rf power. The relatively slow atomic oxygen beam produced in this manner had a measured peak velocity of 1.13×10^5 cm/s and a Mach number of 3.9, which corresponds to a FWHM velocity spread of 41%. The molecular oxygen was 80% dissociated under the operating conditions described above for the 10% O_2–Ar gas mixture, and was free of any $O(^1D_2)$ content as determined by titration with a crossed beam of molecular hydrogen.[18] A 500 V/cm ion deflecting field was placed prior to the interaction zone of the scattering chamber in order to eliminate any interference from ions present in the atomic beam. For both the high and low energy experiments the oxygen beam was collimated to an angular divergence of 2.2° by collimating elements placed after the source skimmer.

The benzene beam was run neat for these experiments at the room temperature vapor pressure of about 90 Torr. The benzene reservoir was immersed in an oil bath in order to eliminate temperature fluctuations. The entire glass line leading from the benzene reservoir to the beam source was heated to at least 10 K above the bath temperature in order to prevent condensation of benzene in the gas line. The nozzle tube and tip were heated to 326 K, as determined by chromel–alumel thermocouples, again in order to prevent condensation from occurring and to eliminate any benzene dimers or higher polymers from being present in the terminal beam. A pure, slightly heated benzene beam was chosen when preliminary testing of a 300 Torr, saturated benzene–argon beam produced extensive dimer formation. See also Ref. 19 for further information about this dimerization phenomena. The benzene beam produced in this manner was found to have a peak velocity of 5.18×10^4 cm/s and a Mach number of 5.8, which corresponds to a FWHM velocity spread of 33%. The similar beam of perdeuterated benzene C_6D_6, obtained from Aldrich Chemical Company with 99.5 atom percent deuterium content, had a peak velocity of 5.14×10^4 cm/s and a Mach number of 4.9 (36% FWHM).

Initially, the most probable collision energies for both the $O + C_6H_6$ and $O + C_6D_6$ systems were 6.5 kcal/mol (O_2 seeded in helium) and 2.5 kcal/mol (O_2 seeded in argon). The angular distributions shown in the next section were obtained at these energies. In subsequent experiments slightly different beam conditions were employed ($\bar{v}_0 = 2.25\times10^5$ cm/s, $\bar{v}_{C_6H_6} = 5.30\times10^4$ cm/s, and $\bar{v}_{C_6D_6} = 5.25\times10^4$ cm/s) which resulted in somewhat higher mean collision energies than those described above: 8.5 kcal/mol for $O + C_6H_6$ and 8.6 kcal/mol for $O + C_6D_6$. The time-of-flight distributions presented later in this paper were recorded for collisions at these higher energies.

Laboratory angular distributions were obtained by taking several scans of 60 s counts at each angle, with time normalization employed when warranted. The supersonic oxygen beam was modulated at 150 Hz with a tuning fork chopper and the number density data at each angle was obtained by subtracting the chopper-closed count from the chopper-open count. Product counting rates at the center-of-mass angle for $m/e = 65$, the predominant mass peak for the C_6H_6 reaction, were typically 300 and 80 counts/s for the high and low energy experiments, respectively. The $m/e = 70$ signal for the C_6D_6 reaction was similarly found to be 550 and 50 counts/s for the high and low energy deuterated experiments, respectively. The larger counting rates for the high energy experiments are principally the result of the higher intensity of the fast oxygen beam relative to the slow oxygen beam. Ve-

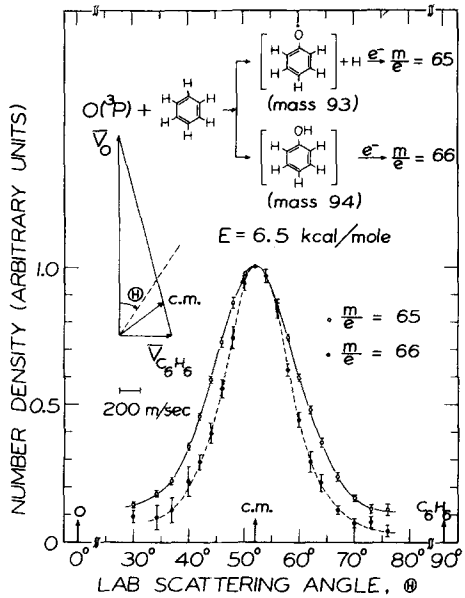

FIG. 1. Angular distributions from the reaction $O(^3P) + C_6H_6$, mean collision energy $E = 6.5$ kcal/mol. The primary reaction products formed were C_6H_5O and C_6H_5OH, which subsequently fragmented during electron bombardment ionization. The solid and dashed lines are drawn through the data for clarity.

locity analysis of the various beams was done with conventional "single shot" time-of-flight techniques. Product time-of-flight distributions were obtained using the cross-correlation time-of-flight technique[20,21] with a 255-bit pseudorandom sequence operated with a 12 μs dwell time per channel. Counting times varied considerably depending upon the laboratory angle and product mass under investigation, with accumulation times of 30 min being representative.

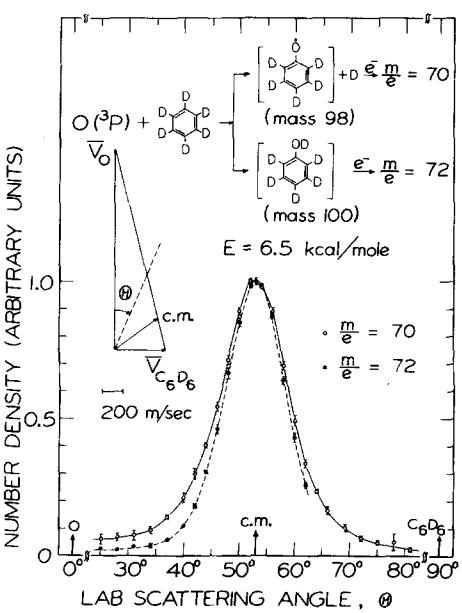

FIG. 2. Angular distributions from the reaction $O(^3P) + C_6D_6$, mean collision energy $E = 6.5$ kcal/mol. The primary reaction products formed were C_6D_5O and C_6D_5OD, which subsequently fragmented during electron bombardment ionization. The solid and dashed lines are drawn through the data for clarity.

TABLE I. Relative intensities of the detected ion masses.

	Mass	Species	Collision energy 6.5 kcal/mol	Collision energy 2.5 kcal/mol
$O + C_6H_6$	94	C_6H_5OH	0.01	< 0.005
	93	C_6H_5O	0.08	0.01
	66	C_5H_6	0.21	0.08
	65	C_5H_5	1.00	1.00
$O + C_6D_6$	100	C_6D_5OD	0.04	< 0.005
	98	C_6D_5O	0.04	< 0.005
	72	C_5D_6	1.05	0.18
	70	C_5D_5	1.00	1.00

RESULTS

Two distinct reaction channels were observed in this study:

$$O(^3P_J) + C_6H_6 \rightarrow C_6H_5O + H, \quad \Delta H^\circ_{298} = -15.9 \text{ kcal/mol}, \quad (1)$$

$$O(^3P_J) + C_6H_6 \rightarrow C_6H_5OH, \quad \Delta H^\circ_{298} = -102.4 \text{ kcal/mol}, \quad (2)$$

with the first channel corresponding to hydrogen elimination and the other to simple oxygen addition, presumably leading ultimately to phenol formation. No direct evidence for CO elimination from the collision complex was found:

$$O(^3P_J) + C_6H_6 \rightarrow C_5H_6 + CO, \quad \Delta H^\circ_{298} = -73.8 \text{ kcal/mol}, \quad (3)$$

where the reaction exoergicity was calculated assuming, for illustrative purposes only, that cyclopentadiene was the C_5H_6 fragment. Similarly, no OH product was detected in these experiments:

$$O(^3P_J) + C_6H_6 \rightarrow C_6H_5 + OH, \quad \Delta H^\circ_{298} = +8.4 \text{ kcal/mol} \quad (4)$$

because the mean collision energies used were insufficient for endothermic abstraction to occur. The atomic oxygen reaction with perdeuterated benzene was found to have the same open product channels as above, although the branching ratio between channels (1) and (2), at a given collision energy, differed significantly from the C_6H_6 reaction.

Figures 1 and 2 show the angular distributions obtained for the high collision energy studies of the $O + C_6H_6$ and $O + C_6D_6$ reactions. The highly excited primary reaction products coming from channels (1) and (2), corresponding to hydrogen elimination (mass 93) and formation of a long-lived collision adduct (mass 94), fragment in the electron bombardment ionizer of our mass spectrometer detector to give $C_5H_5^+$ ($m/e = 65$) and $C_5H_6^+$ ($m/e = 66$) after CO elimination from the parent species during ionization. The daughter ions corresponding to CO elimination from C_6D_5O and C_6D_5OH [respectively, $C_5D_5^+$ ($m/e = 70$) and $C_5D_6^+$ ($m/e = 72$)] were also the major fragment ions of the perdeuterated benzene reaction. The parent ions at masses 94 and 93 for C_6H_6 and masses 100 and 98 for C_6D_6 were also directly observed, but were of much lower intensity than their respective daughter ions. The higher intensity of the daughter fragment ions made them the preferred masses for measuring both the angular and velocity distributions of the parent molecules. This can be seen from the relative intensities shown in Table I. The narrow angular distribu-

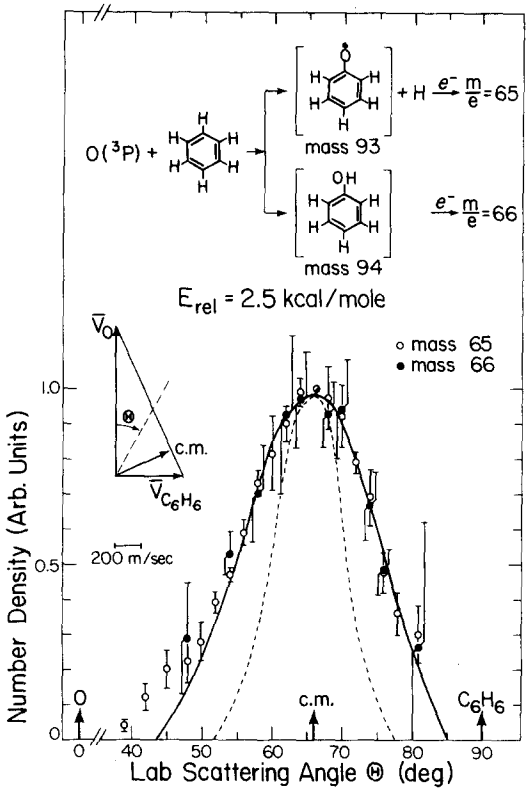

FIG. 3. Angular distributions from the reaction $O(^3P) + C_6H_6$, relative collision energy $E_{rel} = 2.5$ kcal/mol. The dashed line is a calculation of the centroid distribution. The solid line is the calculated distribution described in the text.

tions shown in Figs. 1 and 2 peak around their center-of-mass directions. Masses 66 and 72, corresponding to the addition channel products, have FWHM angular spreads of 14° and 13°, respectively. These distributions can be virtually reproduced by convoluting the finite velocity and angular spreads of the reactant beams with the resolution parameters of the detector. This indicates that the addition channel angular distributions follow the laboratory centroid distributions of the two reactive systems, demonstrating that the ions at masses 66 and 72 are predominantly daughter ions from the addition products C_6H_6O and C_6D_6O.

The wider angular distributions of masses 65 and 70, having FWHM angular spreads of 19° and 15°, respectively, must be attributed to the emission of a particle, i.e., hydrogen or deuterium from the collision complex. These differences in angular distribution widths between masses 65 and 66, and masses 70 and 72, rule out the possibility that the fragment ions having $m/e = 65$ and 70 arise entirely from fragmentation of the same parent species as masses 66 and 72. The narrow spread of the mass 65 and 70 angular distributions also precludes their formation by elimination of the relatively massive CO molecule from the collision complex as conservation of linear momentum would result in a much broader distribution. In subsequent high energy experiments the mass 93 and 98 parent ion angular distributions were obtained, and were found to be in good agreement with the mass 65 and 70 distributions. This provides definitive proof that at a mean collision energy of 6.5 kcal/mol hydrogen elimination constitutes one of the two major open channels for the reaction of ground state atomic oxygen with benzene.

The product angular distributions of the low energy collision experiments are shown in Figs. 3 and 4. The mass 65 and 66 curves of Fig. 3 are superimposable within the uncertainty of the measurements (the error bars in Figs. 1–4 correspond to 95% confidence limits) and the distributions are seen to be broader than the spread in the centroid (dashed line). The yield of C_6H_6O must be very small at this low energy or the mass 66 fragment would be more narrowly distributed than mass 65 from C_6H_5O. In fact, the ratio of the intensity of mass 66 to mass 65 is approximately what would be expected from the ratio of $^{12}C_4{}^{13}CH_5$ to $^{12}C_5H_5$ based on the natural isotopic abundance of ^{12}C and ^{13}C, verifying that at this collision energy the hydrogen elimination product is the only major channel. The data is fit rather well (solid line) by a calculation in which the C_6H_5O product distribution is assumed to be isotropic and the product translational energy distribution is as shown in Fig. 5. The fraction of the available energy appearing in translation is quite high, the average being about 40%. In the absence of an exit channel barrier, a much smaller fraction (< 15%) of the energy is expected from statistical calculations. It is reasonable then to conclude that there is a potential barrier in the exit channel, probably 3–5 kcal/mol. The low energy mass 70 distribution is qualitatively similar to the $O + C_6H_6$ results. An accurate

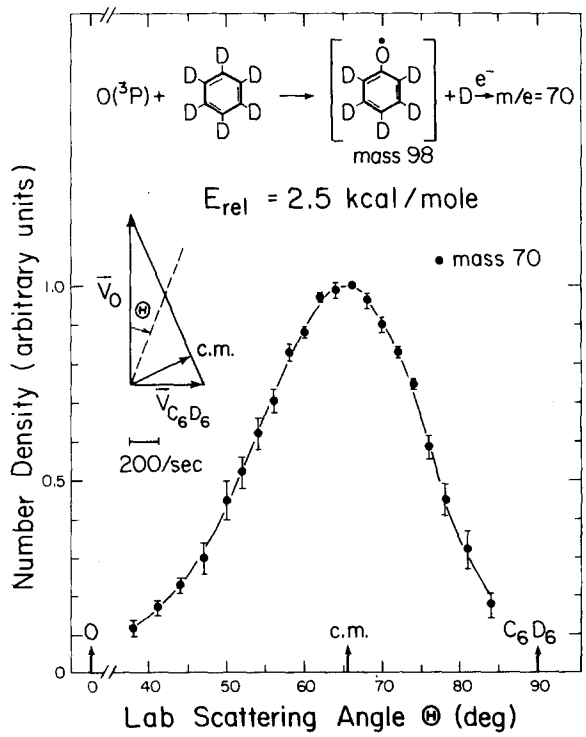

FIG. 4. Angular distribution from the reaction $O(^3P) + C_6D_6 \rightarrow C_6D_5O + D$, $E_{rel} = 2.5$ kcal/mol. Data corresponding to the addition channel could not be obtained due to the presence of an $m/e = 72$ contaminant in the C_6D_6 beam. A line is drawn through the data points for clarity.

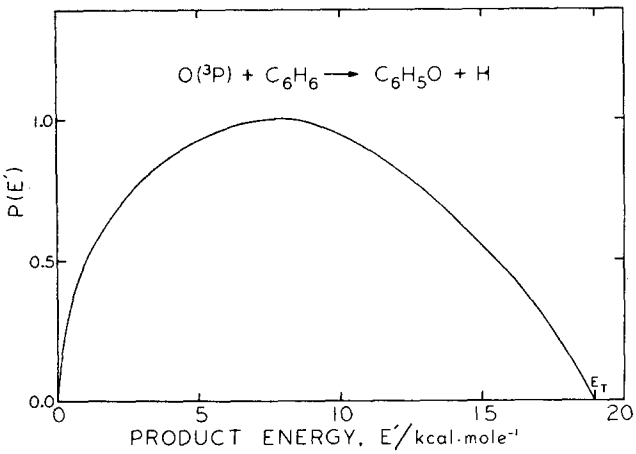

FIG. 5. Translational energy distribution of the product from the reaction $O(^3P) + C_6H_6$, $E_{rel} = 2.5$ kcal/mol.

angular scan of mass 72 could not be obtained here due to the presence of a slight mass 72 impurity in the secondary (perdeuterobenzene) beam. Elastic scattering of this impurity greatly perturbed the wide angle shape of the reactive distribution. This impurity was also present during the high energy $O + C_6D_6$ experiments, but was of little concern since the high energy mass 72 reactive signal was much larger than the elastic signal. The high energy mass 72 reactive signal was in fact more than 50 times larger than the low energy reactive signal (580 versus 10 counts/s).

In Table I are shown the relative intensities of the detected ion masses, accurate to within 10%. These values are the relative signal levels for each system taken at their respective center-of-mass angle. It is immediately obvious that the branching ratio between channels (1) and (2) is dependent on both collision energy and isotopic substitution. If we assume that mass 94 (100) fragments in the electron bombardment ionizer to give roughly equal amounts of masses 66 (72) and 65 (70) while mass 93 (98) fragments to yield predominantly mass 65 (70), then the results shown in Figs. 1–3 and in Table I form a consistent picture of the $O + C_6H_6$ (C_6D_6) reaction. The above fragmentation scheme implies that the observed signal at $m/e = 65$ (70) is a composite of both the addition and elimination channels. For reaction conditions which strongly favor channel 1 (addition) over channel 2 (elimination) the measured daughter ion distributions should be quite similar. This explains the narrow width of the mass 70 angular distribution shown in Fig. 2 because the high energy $O + C_6D_6$ system does, in fact, have a relatively large amount of the addition product. From Table I we can conclude that, for a given collision energy, there is more of the addition product formed in the C_6D_6 reaction than there is in the C_6H_6 reaction, and that increasing collision energy tends to favor the addition channel over the elimination channel. The assumed branching ratio for mass 94 fragmentation in the above argument is based on the observed fragmentation pattern of ground state phenol.[22] The proposed fragmentation of mass 93 to yield predominantly $m/e = 65$ is based on the relative improbability of losing a mass 27 particle versus a mass 28 particle (CO) during ionization.

When the elimination channel is strongly favored with respect to the addition (phenol forming) channel, the $m/e = 66$ (72) daughter peak will be broadened to reflect the mass 93 (98) distribution because the primary product from the elimination reaction will contribute a small amount of signal at $m/e = 66$ (72). Carbon-13 containing fragments also become important in the limit of low phenol production. The low energy $O + C_6H_6$ data presented in Table I and Fig. 3 is consistent with this description. The mass 65 and 66 angular distributions at 2.5 kcal/mol collision energy were virtually superimposable within the uncertainty of the experiment, and the large ($> 10:1$) $m/e = 65$ to $m/e = 66$ ratio indicates that the primary elementary reaction product was mass 93. These conclusions, taken with those in the preceding paragraph, indicate that the relative intensities shown in Table I do not represent the actual branching ratios for this reaction as the daughter ion signals contain contributions from fragmentation of both the addition and elimination reaction products.

Understanding the energy dependence of the product branching ratio is, at the present time, further complicated by the known presence of $O(^1D_2)$ in the high energy (helium seeded) oxygen beam. Thus, some product from the reaction $O(^1D_2) + C_6H_6$ (C_6D_6) may be contributing to the high collision energy results. Work is currently in progress in an attempt to gauge the relative contribution of this alternative reaction pathway.

We have also carried out velocity analysis of the major observable ion peaks for high energy $O + C_6H_6$ (8.5 kcal/mol) and $O + C_6D_6$ (8.6 kcal/mol) collisions. These results provide what we believe to be compelling evidence for the presence of the hydrogen elimination channel and for the low probability of CO elimination at relatively high collision energies. These results support our earlier conclusions. Figure 6 presents the cross-correlation time-of-flight (TOF) data for the $O + C_6H_6$ system taken near its most probable center-of-mass angle. The spectra shown for $m/e = 93$, 66, and 65 have all been corrected for their respective ion flight times. Three major conclusions can be inferred from this figure. First, the mass 93 and mass 65 spectra agree quite closely, especially at higher velocities and both are broader than the mass 66 spectrum. The parent–daughter relationship of $m/e = 93$ and 65 is thus clearly supported. Next, the $m/e = 66$ distribution peaks at the most probable center-of-mass velocity (5.83×10^4 cm/s) as is expected of the addition product. There is no evidence in these m/e 66 and 65 spectra of a high velocity peak from the CO elimination channel, expected to occur around channel 12 if the product translational energy is estimated from the statistical theory of unimolecular dissociation. In order to determine with greater accuracy the relative magnitude of the CO elimination channel, we have obtained a TOF spectrum at an angle removed from the center of mass angle. At this angle, product from Reaction (3), which is more exoergic and expected to have a broader product angular and velocity distribution, should be relatively more intense.

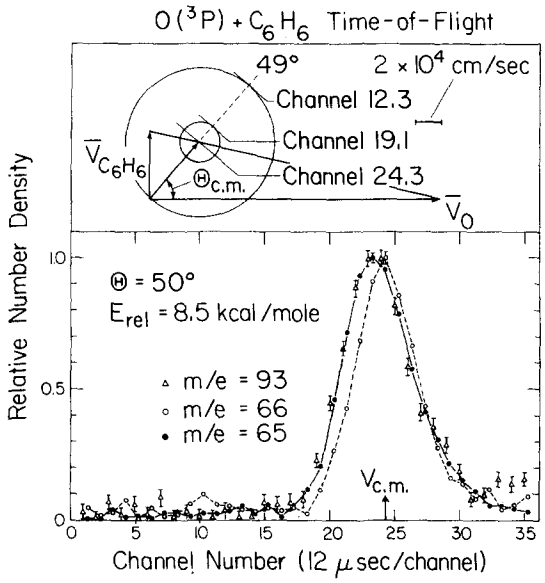

FIG. 6. Product time-of-flight data for the high energy C_6H_6 reaction. All spectra have been corrected for their respective ion flight time offsets. Newton diagram key: larger circle indicates expected mass 66 velocity if 10% of the available energy from the CO elimination channel goes to product translation; smaller circle indicates expected mass 93 velocity if 100% of the available energy from the hydrogen atom elimination channel goes to product translation. Lines are drawn through the data points for clarity.

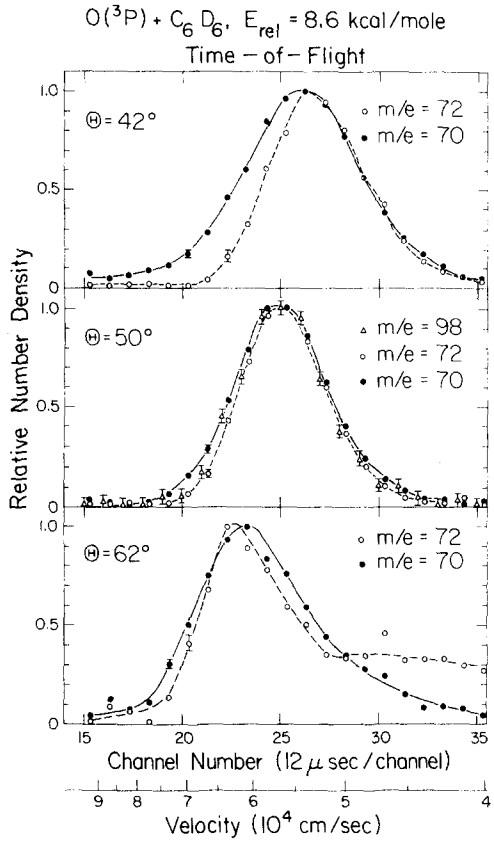

FIG. 8. Product time-of-flight data at three laboratory angles for the high energy C_6D_6 reaction. All spectra have been corrected for ion flight time offsets. Lines are drawn through the data points for clarity.

Shown in Fig. 7 is the TOF spectrum of mass 65 from the high energy reaction at laboratory angle 62° in which a small feature is evident on the fast side of the main product peak. While the source of this small peak may indeed come from the product of Reaction (3), the CO elimination channel, it may also be the contamination from other unknown sources. A calculation in which the cross section for CO elimination is assumed to be 2.5% of that for H elimination is shown to give a reasonably good fit to this fast peak. Several assumptions which were made in order to obtain this comparison include (1) a product translational energy distribution which peaks at 10% of the available energy, (2) a symmetric center of mass angular distribution which peaks on the relative velocity vectors, and (3) equal detection efficiency for product from the two channels (after correctly accounting for center of mass to laboratory transformation Jacobian effects). Assumption (1) and (2) are physically reasonable and probably do not introduce large error to the cross section ratio. Assumption (3) is more difficult to evaluate because the fragmentation pattern of the C_5H_6 product containing 0–80 kcal/mol internal excitation is unknown. Recognizing this limitation we believe with reasonable confidence that the CO elimination channel has a cross section not likely to be more than 5% of the H elimination channel.

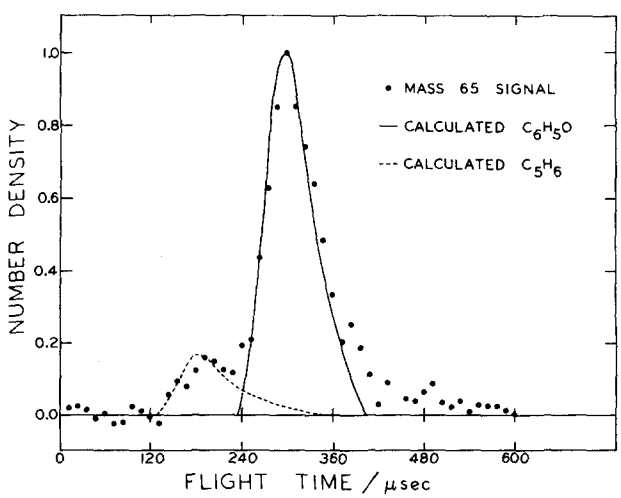

FIG. 7. TOF spectrum of mass 65 product from the reaction of $O + C_6H_6$. The solid line is a calculated distribution of C_6H_5O product. The dashed line is a calculated distribution of C_5H_6 product.

The TOF results for the $O + C_6D_6$ system are shown in Fig. 8. At the center-of-mass angle (50°) the $m/e = 98$, 72, and 70 distributions are seen to peak near channel 25, which corresponds to this system's most probable center-of-mass velocity of $\sim 5.7 \times 10^4$ cm/s. As in the $O + C_6H_6$ reaction, the addition channel daughter ion at $m/e = 72$ is narrower than the elimination channel daughter ion at $m/e = 70$. The parent mass of the elimination channel was also recorded, and is seen to follow the daughter distribution within the uncertainty of the measurement. The absence of any high energy peaks substantiates the estimate that CO

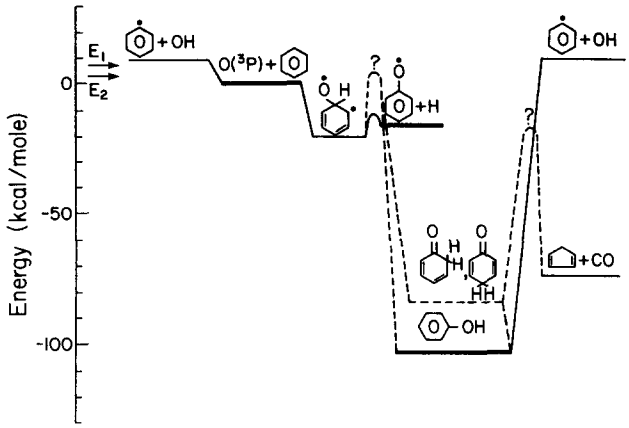

FIG. 9. Energy level diagram of the $O(^3P)$ + benzene reaction. E_1 and E_2 are the two collision energies used in this study.

elimination is less than 5% of the hydrogen elimination. Angle dependent data, shown for $\theta = 42°$ and 62°, were also taken in order to demonstrate the different origins of the $m/e = 72$ and 70 signals. At 42° the larger width of the $m/e = 70$ spectrum relative to the $m/e = 72$ spectrum shows the effects of the deuterium elimination. The low velocity tail of the $m/e = 72$ spectrum at 62° can be attributed to a contaminant effusing from the differential pumping region of the perdeuterobenzene beam.

DISCUSSION

Under single collision conditions the $O(^3P)$ + benzene reactions have been observed to proceed by two distinct elementary reaction pathways. These are the addition of atomic oxygen to benzene to form a long-lived collision adduct, presumably phenol, and the substitution of atomic oxygen for a hydrogen atom. The branching ratio of these two channels has been found to be both isotope and energy dependent, the addition channel being favored with respect to elimination by increased collision energy and by deuterium substitution.

A schematic energy level diagram picturing the important reaction pathways is shown in Fig. 9. The zero of energy in this figure was taken to be the heat of formation of the reactants. The ground state of phenol as well as the CO, OH, and H atom product channels were all located with respect to ground state reactants by their heats of formation.[23-25] The triplet biradical energy level is placed at the level of triplet phenol which is located by the experimentally determined singlet–triplet transition energy observed by Lewis and Kasha,[26] which is in good agreement with the splitting calculated by Dewar and Trinajstic.[27] The ground vibrational level of triplet phenol is stable by about 21 kcal/mol with respect to reactants. The first excited singlet state of phenol S_1 has not been shown in this figure, but is known to fall about 105.8 kcal/mol above S_0, the ground singlet state of phenol.[28,29] The two dashed curves represent energy barriers of unknown magnitude corresponding to the energy needed to access the spin-forbidden triplet–singlet transition, and the barrier to decomposition of singlet phenol to form CO and C_5H_6 (which is represented as cyclopentadiene in the figure). The pyrolysis studies of Cypres and Bettens[30] indicate that the CO and C_5H_6 do in fact correlate with phenol in its singlet ground state. The two most probable collision energies at which we have studied this reaction are indicated by E_1 and E_2 in Fig. 9. Finally, the entrance barrier of the $O(^3P)$ + benzene reaction has not been drawn explicitly, but is thought to be present from the gas phase determination of a 4 kcal/mol activation energy.[12] With this energy level diagram in mind our conceptualization of the reaction mechanism is now presented.

The initial $O(^3P)$ electrophilic attack on benzene probably forms a triplet biradical adduct whose lifetime is believed to be $\lesssim 1$ ns. This highly energetic reaction intermediate can then decay by a variety of channels: It can regenerate the reactants, eliminate a hydrogen atom, or make a radiationless transition to the S_0 manifold of phenol. From statistical considerations, hydrogen elimination from the triplet biradical is expected to dominate oxygen elimination as it is the far more exoergic process. The relatively long lifetime associated with radiative T_1–S_0 phosphorescence precludes its consideration here as a relevant decay channel. Opening of the aromatic ring is also not believed to be a major decay route because the energy threshold is expected to be quite large.

In this study two main reaction channels were actually observed: hydrogen elimination and C_6H_6O formation. Consequently, we view the next step of the reaction mechanism as being a competition between atomic hydrogen elimination from the triplet adduct, and intersystem crossing to internally excited singlet phenol. The deep well and the high density of states of this singlet phenol contribute to a long statistical lifetime ($\gg 1$ ms), which is the approximate flight time to our detector. The very small contribution from the CO elimination is evidence for a large energy barrier to this process. This is not unreasonable as breaking of the aromatic ring probably requires that the complex pass through a highly energetic critical configuration.

The broad product translational energy distribution for the hydrogen elimination channel (Fig. 5) would result from the existence of a small potential barrier (3–5 kcal/mol) in the exit channel. This conclusion is consistent with gas phase studies of H atom addition to alkyl and halobenzenes which have established an activation energy around 4 kcal/mol. The product energy distribution measured here is quite similar to that for the reaction of fluorine atoms with C_6D_6 in which deuterium elimination deposits close to 50% of the available energy in translation.[31]

Examination of the relative product intensities shown in Table I indicates that the branching ratio between the hydrogen elimination and intersystem crossing channels is energy dependent. This is seen by the increase in $m/e = 66$ (72), the addition channel, relative to that of $m/e = 65$ (70), the elimination channel,

as the collision energy is increased from 2.5 to 6.5 kcal/mol. This observation suggests that the T_1–S_0 surface crossing probability increases with increasing energy. Sloane[15] has performed a crude SCF calculation which fixes a T_1–S_0 crossing point at 38 kcal/mol above the minimum energy configuration of T_1 or 10 kcal/mol above the energy of our intermediate. Although this was not a "chemically accurate" value, it bears out the possibility of an energy dependent branching ratio.

Also in question is the actual distribution of total energies present in the reaction intermediate. Several kinetic studies have confirmed the existence of a 4 kcal/mol Arrhenius activation energy in the reaction of $O(^3P)$ with benzene.[12] This implies that a small entrance channel barrier is present in the triplet surface. Thus, although the most probable collision energies are 2.5 and 6.5 kcal/mol, the most probable excitations of the triplet adduct may be greater than these collision energies indicate. This is certainly true for Sloane's[15] crossed effusive beam study as his most probable collision energy was only 0.61 kcal/mol. Apparently, collisions involving molecules in the high energy tails of his Maxwellian distributions were the ones leading to reaction.

The branching ratio of the two channels is also isotope dependent. This is expected as both the rate of hydrogen atom elimination and that of the radiationless T_1–S_0 transition are isotope dependent. The rate of hydrogen elimination is expected to decrease with deuteration from the "primary isotope effect",[32] i.e., the increase in state density and decrease in zero point energy which tend to lower the rate constant.

The effect of deuteration on the intersystem crossing is uncertain particularly because neither the energy of the crossing point nor the dominant vibrational modes which influence the crossing are known. The very strong deuterium effect observed suggests that the rate of intersystem crossing to the S_0 electronic state increases dramatically with deuteration, because the primary isotope effect on the H elimination channel is unlikely to be this large. The possibility of intersystem crossing to the S_1 state followed by rapid radiation decay to the ground state bears further investigation through fluorescence measurements.

Earlier studies of the $O(^3P)$ + benzene reaction had reported that CO elimination was an important reaction pathway.[4,15] Our results indicate that CO elimination, if it is occurring at all, is a relatively minor product channel. The fact that C_6H_6O, which contains ~ 110 kcal of excitation energy, can be detected after 200 μs of flight time, shows that the barrier of $C_6H_6O \rightarrow CO + C_5H_5$ must be as high as 85–90 kcal/mol if the RRKM theory of unimolecular decomposition is applied for the decomposition of C_6H_6O. Of course, if there is no collision to stabilize the excited C_6H_6O, it will eventually decompose to $CO + C_5H_5$ or return to reactant $O + C_6H_6$. However, in a bulk experiment at moderate pressure, the faster collisional stabilization of excited C_6H_6O should dominate over the slower dissociation process. As Boocock and Cvetanovic's experiment[4] was carried out under multiple collision conditions, secondary reactions involving $O(^3P)$ atoms and radical products might be the source of their observed CO. Sloane[15] has postulated that CO elimination was a primary reaction channel based on his observation of a strong $m/e = 66$ signal in his crossed effusive beam experiment, which employed a fixed (nonrotatable) electron bombardment ionizer–quadrupole mass spectrometer. On the basis of the appearance potentials observed for $C_5H_6^+$ (minor threshold at 9.0 eV and major product threshold at 9.6 eV) he proposed that cyclopentadiene was a minor product and that 3-pentene-1-yne was a major product coinciding with CO elimination. Our study has shown that the strong $m/e = 66$ peak results principally from fragmentation of highly excited mass 94 adduct during electron bombardment ionization. As the mass 94 adduct produced in the $O(^3P)$ + benzene reaction has > 102 kcal/mol of internal excitation relative to ground state phenol, it is not surprising that the appearance potential for $C_5H_6^+$ production is shifted to a lower value than that found for internally cool phenol. Although Sloane discussed the above possibility,[15] he concluded that CO elimination was a major reaction pathway. This conclusion is contraindicated by the results of our experiment.

The presence of viscous, polymeric reaction products[4,8] in gas phase studies suggests that radicals are produced in the reaction. Our observation that the phenoxy radical is a major reaction product, especially at low collision energies, supports this contention. Spectroscopic examination of the polymeric residue using IR absorption and NMR suggests the presence of –OH, C–O–C, and –CHO functional groups.[8] Mass spectrometric analysis of the polymeric residue yields many mass peaks, with $m/e = 185$ being most intense.[8] Sequential attack of phenoxy radicals on benzene, could produce a long-chain polymer, which might yield an etherlike substance: $(C_6H_5–O–C_6H_4–O)^*$, $m/e = 185$. This speculation seems plausible as ether linkages have been inferred from IR spectra, phenoxy radicals are known to be present from this study, and $m/e = 185$ was observed in the mass spectrum reported by Bonanno *et al.*

CONCLUSION

The reaction of $O(^3P)$ with benzene has been shown to proceed initially by the addition of atomic oxygen to benzene, presumably forming a triplet biradical intermediate, which subsequently decays by either hydrogen elimination or nonradiative transition to the S_0 manifold of phenol. The branching ratio of these two reaction channels has been found to be both isotope and energy dependent, with the addition channel being favored with respect to elimination for increasing collision energy and deuterium substitutions. Our results confirm that oxygen addition and hydrogen elimination are the major open reaction channels while CO elimination, if occurring at all, is a relatively minor reaction pathway. This study illustrates that crossed molecular beam experiments employing both product velocity and angu-

lar distribution analysis using mass spectrometric particle detection are well suited for unraveling the complex mechanisms of gas phase radical reactions. Advantage is taken of the dynamic and energetic constraints imposed on the reactive products produced in a bimolecular reactive collision. Future studies using our supersonic atomic oxygen beam source will include reactions with aliphatic, olefinic, and other aromatic hydrocarbons in order to arrive at a more complete understanding of atomic oxygen–hydrocarbon reactions.

ACKNOWLEDGMENTS

This work was supported by the Division of Chemical Sciences, Office of Basic Energy Sciences, U.S. Department of Energy under contract No. W-7405-Eng-48 and the Office of Naval Research under contract No. N00014-75-C-0671. S.J.S thanks the Gulf Oil Research Foundation for partial fellowship support. P.C. acknowledges a fellowship from the Italian Ministry of Education and travel support from NATO grant No. 1444.

[1]J. R. Kanofsky and D. Gutman, Chem. Phys. Lett. **15**, 236 (1972).
[2]J. R. Kanofsky, D. Lucas, F. Pruss, and D. Gutman, J. Phys. Chem. **78**, 311 (1974).
[3]J. R. Kanofsky, D. Lucas, and D. Gutman, 14th International Symposium on Combustion (1973), Pittsburgh, Penn., pp. 285–294.
[4]G. Boocock and R. J. Cvetanović, Can. J. Chem. **39**, 2436 (1961).
[5]E. Grovenstein, Jr. and A. J. Mosher, J. Am. Chem. Soc. **92**, 3810 (1970).
[6]I. Mani and M. C. Sauer, Jr., Adv. Chem. Ser. **82**, 142 (1968).
[7]L. I. Avramenko, R. V. Kolesnikova, and G. I. Savinova, Isv. Akad. Nauk. SSSR Ser. Khim. **1**, 28 (1965).
[8]R. A. Bonanno, P. Kim, J.-H. Lee, and R. B. Timmons, J. Chem. Phys. **57**, 1377 (1972).
[9]S. Furuyama and N. Ebara, Int. J. Chem. Kinet. **7**, 689 (1975).
[10]R. Atkinson and J. N. Pitts, Jr., J. Phys. Chem. **78**, 1780 (1974).
[11]A. J. Colussi, D. L. Singleton, R. S. Irwin, and R. J. Cvetanović, J. Phys. Chem. **79**, 1900 (1975).
[12]R. Atkinson and J. N. Pitts, Jr., Chem. Phys. Lett. **63**, 485 (1979).
[13]J. C. Chu, H. C. Ai, and D. F. Othmer, Ind. Eng. Chem. **45**, 1266 (1953).
[14]R. E. Huie and J. T. Herron, in *Progress in Reaction Kinetics*, edited by K. R. Jennings and R. B. Cundall (Pergamon, Oxford, 1975), Vol. 8, pp. 60–63.
[15]T. M. Sloane, J. Chem. Phys. **67**, 2267 (1977).
[16]Y. T. Lee, J. D. McDonald, P. R. LeBreton, and D. R. Herschbach, Rev. Sci. Instrum. **40**, 1402 (1969).
[17]S. J. Sibener, R. J. Buss, and Y. T. Lee, XIth International Symposium on Rarefied Gas Dynamics, Cannes, France (1979), Vol. II, pp. 981–990.
[18]S. J. Sibener, R. J. Buss, and Y. T. Lee, Rev. Sci. Instrum. **51**, 167 (1980).
[19]K. C. Janda, J. C. Hemminger, J. S. Winn, S. E. Novick, S. J. Harris, and W. Klemperer, J. Chem. Phys. **63**, 1419 (1975).
[20]V. L. Hirschy and J. P. Aldridge, Rev. Sci. Instrum. **42**, 381 (1971).
[21]K. Sköld, Nucl. Instrum. Meth. **63**, 114 (1968).
[22]*Atlas of Mass Spectral Data*, edited by E. Stenhagen, S. Abrahamsson, and F. W. McLafferty (Interscience, New York, 1969), Vol. **1**, p. 48.
[23]S. W. Benson, *Thermochemical Kinetics* (Wiley, New York, 1976), 2nd edition.
[24]H. M. Rosenstock, K. Draxl, B. W. Steiner, and J. T. Herron, J. Phys. Chem. Ref. Data **6**, 774 (1977).
[25]A. J. Colussi, F. Zabel, and S. W. Benson, Int. J. Chem. Kinet. **9**, 161 (1977).
[26]G. N. Lewis and M. Kasha, J. Am. Chem. Soc. **66**, 2100 (1944).
[27]M. J. S. Dewar and N. Trinajstic, J. Chem. Soc. A **9**, 1220 (1971).
[28]H. J. Teuber and W. Schmidtke, Chem. Ber. **93**, 1257 (1960).
[29]H. Zimmerman and N. Joop, Z. Electrochem. **65**, 61 (1961).
[30](a) R. Cypres and B. Bettens, Tetrahedron **30**, 1253 (1974); (b) R. Cypres and B. Bettens, Tetrahedron **31**, 359 (1975).
[31]K. Shobatake, J. M. Parson, Y. T. Lee, and S. A. Rice, J. Chem. Phys. **59**, 1427 (1973).
[32]W. Forst, *Theory of Unimolecular Reactions* (Academic, New York, 1973), p. 350.